Sensors and Materials, Vol. 31, No. 4 (2019) 1257–1264
MYU Tokyo

S & M 1852

Scintillation and Dosimetric Properties of Sn-doped ZnO-SiO_2-B_2O_3 Glasses

Noriaki Kawaguchi* and Takayuki Yanagida

Nara Institute of Science and Technology, 8916-5 Takayama-cho, Ikoma, Nara 630-0192, Japan

(Received December 3, 2018; accepted April 4, 2019)

Keywords: dosimeter, luminescence, glass

We have studied the scintillation and dosimetric properties of Sn-doped ZnO-SiO_2-B_2O_3 glasses. The glass samples were obtained by a conventional melt quenching method. In the scintillation spectra of the Sn-doped ZnO-SiO_2-B_2O_3 glasses, emission peaks due to the 5p → 5s transition of Sn^{2+} ions were observed. Scintillation decay times of the Sn-doped ZnO-SiO_2-B_2O_3 glasses were from 2.44 to 2.95 μs. In the thermoluminescence (TL) glow curves of the Sn-doped ZnO-SiO_2-B_2O_3 glasses, we observed broad glow peaks at 200 °C. From the dose–response curve, the lower limit of detection for the 0.1% Sn-doped sample was 0.1 mGy.

1. Introduction

Ionizing radiation has many industrial, medical, and scientific applications. In these applications, radiation measurement techniques using the scintillator[1–3] and dosimetric materials play an important role. Scintillators have a function to convert ionizing radiation to visible light immediately and are suitable for online measurements. Dosimetric materials can be classified as thermoluminescence (TL),[4] optically stimulated luminescence (OSL),[5–8] and radio-photoluminescence (RPL)[9–13] materials. These three types of materials, which have three different luminescent mechanisms, are used for long-term dose monitoring.

Scintillators are required to have a high light yield, a fast decay time, and a high discrimination capability. The energy resolution of the scintillation detector depends on the light yield of the scintillator. The fast response of the scintillation detector can be realized by the fast decay time of the scintillator. To discriminate ionizing radiations, the effective atomic number (Z_{eff}) of the scintillator for γ-ray detection is important because heavy elements can interact with γ-rays efficiently. On the other hand, the scintillators for thermal neutron and charged-particle detection are required to consist of light elements to decrease the rate of erroneous detection by the interaction with γ-rays. In addition, the thermal neutron scintillator has to contain specific elements having high cross sections for the (n, α) and (n, γ) nuclear reactions (e.g., ^{6}Li or ^{10}B). The conventional scintillators for γ-ray and thermal neutron detection were reviewed by van Eijk,[2] who comprehensively covered, for example, Tl:NaI,

*Corresponding author: e-mail: n-kawaguchi@ms.naist.jp
https://doi.org/10.18494/SAM.2019.2185

ISSN 0914-4935

$Bi_4Ge_3O_{12}$, Tl:CsI, Ce:Gd_2SiO_5, and Ce:Lu_2SiO_5 as γ-ray scintillators, and Eu:LiI, LiF/Ag:ZnS, and GS20 (Ce-doped lithium silicate glass) as thermal neutron scintillators. Among all the reviewed scintillators, only GS20 is the glass material.

The required properties of dosimetric materials are a linear response to a wide dose range, a tissue equivalency, and a low fading rate for a recorded dose. The required measurable dose range depends on the application, but the lower limits of detection by commercial materials are typically from 0.01 to 0.1 mGy in personal dosimetry. The tissue equivalency depends on the composition of the dosimetric material, and the effective atomic number of H_2O is ideal because it is close to the human tissue. The low fading rate is realized by the TL and OSL dosimetric materials with high glow peak temperatures, and the RPL dosimetric materials are considered to have low fading rates owing to their luminescent mechanism. As the TL dosimetric materials, Mg, Ti:LiF, Mn:CaF_2, Dy:CaF_2, and Tm:$CaSO_4$ are used. The well-known OSL dosimetric materials are C:Al_2O_3 and BeO. The Ag-doped phosphate glass is practically used as the RPL dosimetric material. Among them, only the RPL dosimetric material is glass.

Over the past few decades, both scintillators and dosimetric materials have been intensively studied; however, there are few glass materials in practical use. Since glass materials are potentially cost-effective to produce and it is easy to control their size and shape, we are interested in the scintillation and dosimetric properties of glass materials. Since it has been reported that Sn-doped zinc phosphate glasses show high quantum yields,[14–17] the scintillation and dosimetric properties of the Sn-doped ZnO-P_2O_5, Li_2O-B_2O_3-SiO_2, SrO-B_2O_3, and $Zn_3(PO_4)_2$-$NaPO_3$ glasses have been studied.[18–25] It is confirmed that these glasses show scintillation, TL, and OSL. In particular, the Sn-doped ZnO-P_2O_5 and $Zn_3(PO_4)_2$-$NaPO_3$ glasses show good properties; thus, the scintillation and dosimetric properties of other Sn-doped ZnO-based glasses are our recent interest. In addition, the scintillation and dosimetric properties of Sn-doped zinc borosilicate glasses have not been studied, although borosilicate glasses are widely used for many applications owing to their high chemical stability and transparency. In this work, we have studied the scintillation and dosimetric properties of the Sn-doped ZnO-SiO_2-B_2O_3 glasses.

2. Materials and Methods

The undoped and ZnO-SiO_2-B_2O_3 glasses were prepared by the conventional melt quenching method. High-purity SnO_2, ZnO, SiO_2, and B_2O_3 powders were used as the starting materials, which were mixed in the mole ratios of $x$$SnO_2$-40ZnO-30$SiO_2-30B_2O_3$ (x = 0, 0.1, 0.5, 1.0, 2.0, and 5.0). The mixed powders were melted in alumina crucibles at 1450 °C for 30 min in air atmosphere using an electric furnace (FTV-1700, FULL-TECH). The melted mixtures were quenched on a stainless plate preheated at 300 °C and pressed by another stainless plate. The obtained glasses were cut and mechanically polished into 1 mm thickness before the measurements described below.

In-line transmittance spectra were measured using a spectrophotometer (V-670, JASCO) across a spectral range between 190 and 2700 nm with 1 nm steps. Photoluminescence (PL) excitation and emission maps and PL quantum yields were measured using a PL spectrometer

(Quantaurus-QY, Hamamatsu Photonics). The spectral ranges of excitation and emission were the wavelength ranges from 250 to 400 nm and 200 to 900 nm, respectively.

X-ray-induced scintillation spectra were measured using our experimental setup consisting of an X-ray generator, an optical fiber, and a spectrometer. The samples were irradiated by X-rays from the generator equipped with a conventional X-ray tube with a tungsten anode target and a beryllium window (XRB80P&N200X4550, Spellman), and their luminescences were guided to a monochromator (Shamrock 163, Andor) equipped on a CCD-based spectrometer (DU920-BU2NC, Andor) in order to measure the emission spectra. The applied tube voltage and current were 80 kV and 1.2 mA, respectively. The X-ray-induced scintillation decay times were measured using a time-correlated single-photon counting system operated together with a pulse X-ray source. The X-ray tube voltage was 30 kV, and a photomultiplier tube (R7400P-06, Hamamatsu Photonics) was also used to detect the signal. The system offers a time resolution of a few nanoseconds. The obtained decay curves were fitted by

$$I(t) = A \exp(-t/\tau) + C, \tag{1}$$

where $I(t)$ is the luminescence intensity as a function of time t, τ is the scintillation decay time, and A and C are constants.

To investigate the dosimetric properties, TL glow curves were measured using a TL reader (TL-2000, Nanogray Inc.) by heating the samples at a rate of 1 °C/s in the temperature range from 50 to 490 °C. Prior to the measurement, the glass samples were irradiated with X-rays at certain doses. The measurements were repeated with several different irradiation doses from 0.1 mGy to 10 Gy to obtain dose–response curves, which indicate relationships between the TL emission intensities and the corresponding irradiation doses, and are one of the important properties of dosimetric materials.

3. Results and Discussion

Figure 1 shows aspects of the cut and polished Sn-doped ZnO-SiO_2-B_2O_3 glass samples. All the samples have no visible cracks and the Sn-doped samples show luminescence under UV

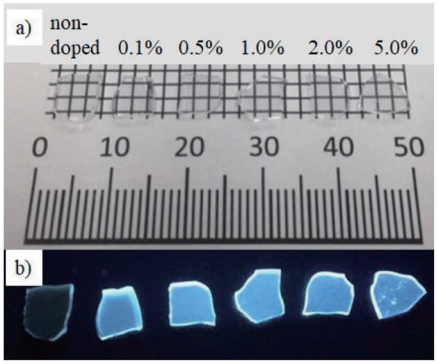

Fig. 1. (Color online) Undoped and Sn-doped ZnO-SiO_2-B_2O_3 glasses under (a) ambient and (b) 254 nm UV light.

irradiation. Figure 2 shows the transmittance spectra of the samples. The transmittances of the samples in the wavelength range from 400 to 2700 nm are from 70 to 90%. The transparencies of all the samples are acceptable as scintillators and dosimeter materials.

Figure 3 shows the PL excitation and emission maps of the undoped and 1.0% Sn-doped samples. In the 1.0% Sn-doped sample, the broad emission from 300 to 700 nm peaking at 420 nm with excitation wavelengths from 250 to 350 nm was observed. This emission can be ascribed to the 5p → 5s transition of Sn^{2+} ions. We cannot observe any PL peaks from the undoped sample. Figure 4 shows the dopant concentration dependence of the maximum PL quantum yields of the Sn-doped samples. The maximum PL quantum yields of the Sn-doped samples were from 11 to 29%, and the 1.0% Sn-doped sample showed the highest quantum yield.

Figure 5 shows the X-ray-induced scintillation spectra of the undoped and Sn-doped samples. In the Sn-doped samples, broad emissions from 300 to 700 nm were observed, whereas a weak and broad emission peak was observed in the undoped sample. It is considered that the emissions in the Sn-doped samples are ascribed to the 5p → 5s transition of Sn^{2+} ions similarly to PL. The origin of the emission in the undoped samples is unclear, but it may be due to some

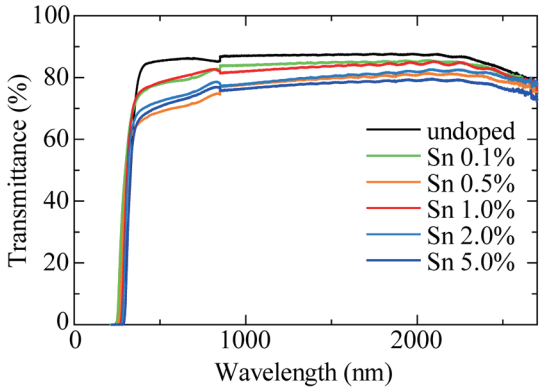

Fig. 2. (Color online) Transmittance spectra of undoped and Sn-doped $ZnO\text{-}SiO_2\text{-}B_2O_3$ glasses.

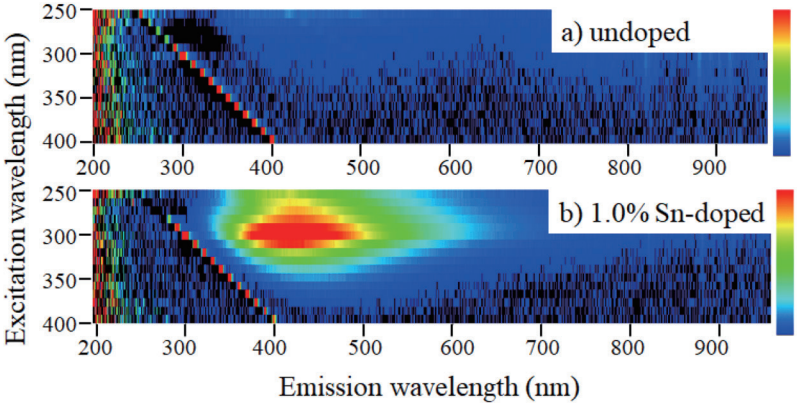

Fig. 3. (Color online) PL excitation and emission maps of undoped and 1.0% Sn-doped $ZnO\text{-}SiO_2\text{-}B_2O_3$ glasses.

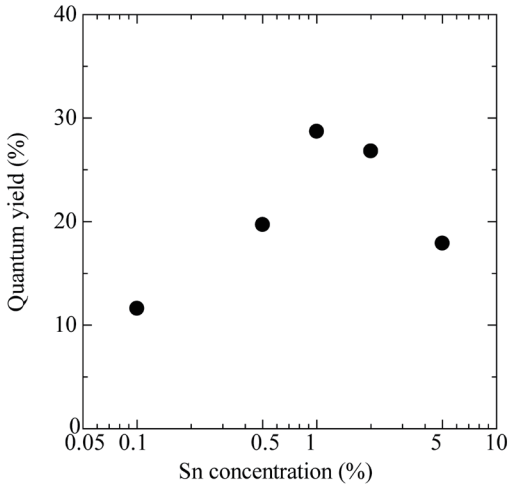

Fig. 4. Dopant concentration dependence of maximum PL quantum yields of Sn-doped ZnO-SiO_2-B_2O_3 glasses.

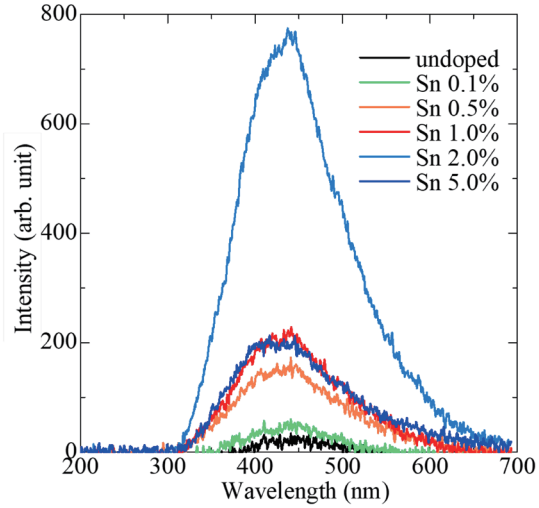

Fig. 5. (Color online) X-ray-induced scintillation spectra of undoped and Sn-doped ZnO-SiO_2-B_2O_3 glasses.

kind of defect luminescence. Such intrinsic defect luminescence of inorganic compounds is often observed in the scintillation spectra. Figure 6 shows the X-ray-induced scintillation decay curves of the 0.5, 1.0, 2.0, and 5.0% Sn-doped samples. The X-ray-induced scintillation decay curves of the undoped and 0.1% Sn-doped samples could not be measured owing to their low luminescence intensities. The scintillation decay curve was fitted to a single-component exponential decay. The decay times of the samples were from 2.44 to 2.95 μs, which are shown in Table 1. The obtained decay times are consistent with those of luminescence with the 5p → 5s transition of Sn^{2+} ions. The decay times of the samples are acceptable for many scintillator applications, but the scintillation intensities are insufficient owing to their lower PL quantum yields than commercial materials. In general, the scintillation light yield is affected by the conversion process of radiation to electron-hole pairs, the transport efficiency of electron-hole pairs, and the quantum efficiency of the luminescent centers. Commonly used scintillators at least have to show a high PL quantum yield, which is related to the quantum efficiency at the luminescent centers.

Figure 7 shows the TL glow curves of the undoped and Sn-doped samples. Although the undoped sample shows a weak glow peak, the Sn-doped samples show significantly higher TL intensities, and the highest intensity is observed in the 0.1% Sn-doped sample. The TL glow peaks of the Sn-doped samples are around 200 °C and their peak temperatures are similar to those of commercial TL dosimetric materials, but they have large peak widths and show TL also at low temperatures. The TL intensity decreases with increasing Sn concentration, which is a different tendency from the Sn concentration dependence of the scintillation intensity. In our opinion, the reason for this difference is that both scintillation and TL intensities are affected by the trapping centers in the samples. The TL is caused by the recombination of electrons and holes released from the trapping centers; therefore, the TL intensity tends to increase with the

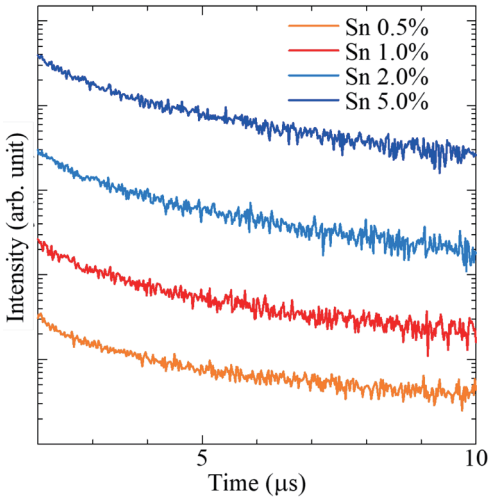

Fig. 6. (Color online) X-ray-induced scintillation decay curves of 0.5, 1.0, 2.0, and 5.0% Sn-doped $ZnO\text{-}SiO_2\text{-}B_2O_3$ glasses.

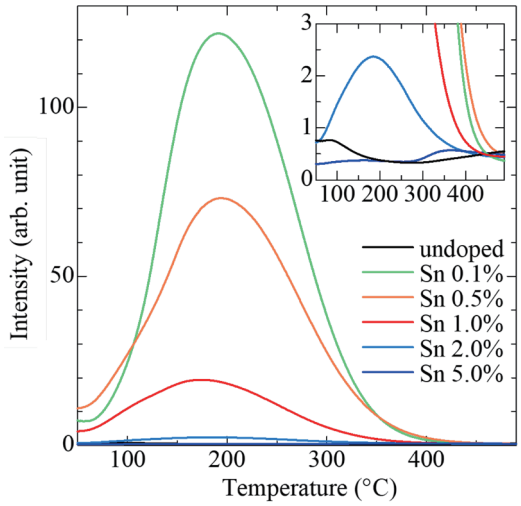

Fig. 7. (Color online) TL glow curves of undoped and Sn-doped $ZnO\text{-}SiO_2\text{-}B_2O_3$ glasses.

Table 1
Scintillation decay times of Sn-doped $ZnO\text{-}SiO_2\text{-}B_2O_3$ glasses.

Sn concentration (%)	Scintillation decay time (ms)
0.5	2.57
1.0	2.44
2.0	2.62
5.0	2.95

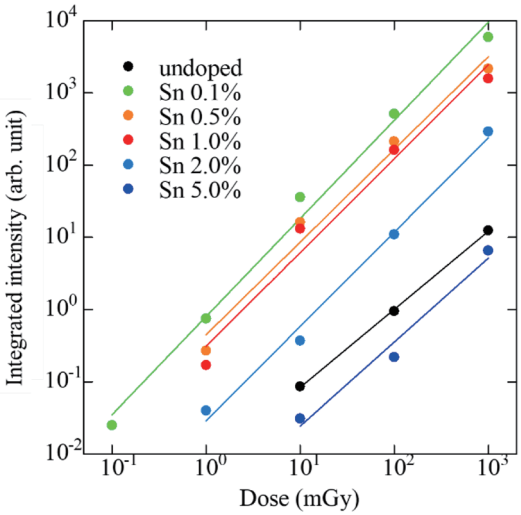

Fig. 8. (Color online) TL dose–response curves of undoped and Sn-doped $ZnO\text{-}SiO_2\text{-}B_2O_3$ glasses.

trap concentration. In contrast, the scintillation intensity decreases with an increase in trap concentration since the transport of electron-hole pairs is interfered by the trapping centers. In the case of the Sn-doped samples, the trap concentration is assumed to decrease with increasing Sn concentration. In addition, the difference in optimal Sn concentration for the PL quantum yields and scintillation intensities can also be explained by using the trap concentration. In Figs. 4 and 5, the optimal Sn concentration for the scintillation intensities becomes higher than that for the PL quantum yields owing to the lower transport efficiency of electron-hole pairs in the samples with lower Sn concentrations. Figure 8 shows the TL dose–response curves of the undoped and Sn-doped samples. The widest measurable range among the samples is shown by

the 0.1% Sn-doped sample having the highest TL intensity among the samples. The lower limit of detection using the 0.1% Sn-doped sample is 0.1 mGy, which is acceptable compared with those of commercial materials.

4. Conclusions

The scintillation and dosimetric properties of Sn-doped ZnO-SiO_2-B_2O_3 glasses have been studied. The glass samples were obtained by the conventional melt quenching method. The 0.1% Sn-doped sample showed a broad emission from 300 to 700 nm, peaking at 420 nm with excitation wavelengths from 250 to 350 nm, whereas the undoped sample showed no PL peaks. The PL emission from the 0.1% Sn-doped sample can be ascribed to the 5p → 5s transition of Sn^{2+} ions. The maximum PL quantum yields of the Sn-doped samples were from 11 to 29%. Scintillation spectra of the Sn-doped samples showed emission peaks due to the 5p → 5s transition of Sn^{2+} ions similarly to the PL spectrum of the 0.1% Sn-doped sample. From the scintillation decay curves of the Sn-doped samples, their scintillation decay times were from 2.44 to 2.95 μs. From the TL glow curves of the Sn-doped samples, broad glow peaks were observed at 200 °C. All the samples showed linear dose–response curves in the various dose ranges. The lower limit of detection for the 0.1% Sn-doped sample was 0.1 mGy, which is the lowest among those for all the samples.

Acknowledgments

This work was supported by a Grant-in-Aid for Scientific Research (A)-26249147 and a Grant-in-Aid for Research Young Scientists (18K14158) from the Ministry of Education, Culture, Sports, Science and Technology of the Japanese government (MEXT), as well as by the A-STEP and Matching Planner Program of the Japan Science and Technology Agency (JST). The Cooperative Research Project of the Research Institute of Electronics, Shizuoka University, Izumi Science and Technology Foundation, Iwatani Naoji Foundation, Kazuchika Okura Memorial Foundation, and Terumo Foundation for Life Sciences and Arts are also acknowledged.

References

1 G. F. Knoll: Radiation Detection and Measurement (Wiley, New York, 2010) 4th ed.
2 C. W. E. van Eijk: Nucl. Instrum. Methods Phys. Res., Sect. A **460** (2001) 1.
3 T. Yanagida: Opt. Mater. **35** (2013) 1987.
4 S. W. S. McKeever: Thermoluminescence of Solids (Cambridge University Press, Cambridge, 1985).
5 E. G. Yukihara and S. W. S. McKeever: Optically Stimulated Luminescence (Wiley, Chichester, UK, 2011).
6 S. W. S. McKeever: Nucl. Instrum. Methods Phys. Res., Sect. B **184** (2001) 29.
7 G. Okada, K. Fukuda, S. Kasap, and T. Yanagida: Photonics **3** (2016) 23.
8 N. M. Winch, A. Edgar, and C. M. Bartle: Nucl. Instrum. Methods Phys. Res., Sect. A **763** (2014) 394.
9 H. Nanto, Y. Miyamoto, T. Oono, Y. Takei, T. Kurobori, and T. Yamamoto: Procedia Eng. **25** (2011) 231.
10 G. Okada, B. Morrell, C. Koughia, A. Edgar, C. Varoy, G. Belev, T. Wysokinski, D. Chapman, and S. Kasap: Appl. Phys. Lett. **99** (2011) 121105.
11 G. Okada, J. Ueda, S. Tanabe, G. Belev, T. Wysokinski, D. Chapman, D. Tonchev, and S. Kasap: J. Am. Ceram. Soc. **97** (2014) 2147.

12 Y. Miyamoto, H. Nanto, T. Kurobori, Y. Fujimoto, T. Yanagida, J. Ueda, S. Tanabe, and T. Yamamoto: Radiat. Meas. **71** (2014) 529.
13 G. Okada, Y. Fujimoto, H. Tanaka, S. Kasap, and T. Yanagida: J. Rare Earths **34** (2016) 769.
14 H. Masai, Y. Takahashi, T. Fujiwara, S. Matsumoto, and T. Yoko: Appl. Phys. Express **3** (2010) 082102.
15 H. Masai, T. Tanimoto, S. Okumura, K. Teramura, S. Matsumoto, T. Yanagida, Y. Tokuda, and T. Yoko: J. Mater. Chem. C **2** (2014) 2137.
16 H. Masai, A. Koreeda, Y. Fujii, T. Ohkubo, and S. Kohara: Opt. Mater. Express **6** (2016) 1827.
17 A. Torimoto, H. Masai, G. Okada, T. Yanagida, and M. Koshimizu: Sens. Mater. **29** (2017) 1383.
18 H. Masai, T. Yanagida, Y. Fujimoto, M. Koshimizu, and T. Yoko: Appl. Phys. Lett. **101** (2012) 191906.
19 T. Yanagida, Y. Fujimoto, T. Ito, K. Uchiyama, and K. Mori: Appl. Phys. Express **7** (2014) 062401.
20 H. Masai, Y. Suzuki, T. Yanagida, and K. Mibu: Bull. Chem. Soc. Jpn. **88** (2015) 1047.
21 H. Nanto, R. Nakagawa, Y. Takei, K. Hirasawa, Y. Miyamoto, H. Masai, T. Kurobori, T. Yanagida, and Y. Fujimoto: Nucl. Instrum. Meth. Phys. Res., Sect. A **784** (2015) 14.
22 H. Masai, Y. Ueda, T. Yanagida, G. Okada, and Y. Tokuda: Sens. Mater. **28** (2016) 871.
23 H. Masai, T. Yanagida, G. Okada, A. Koreeda, and T. Ohkubo: Sens. Mater. **29** (2017) 1391.
24 A. Torimoto, H. Masai, G. Okada, and T. Yanagida: Radiat. Meas. **106** (2017) 175.
25 S. Hirano, N. Kawano, G. Okada, N. Kawaguchi, and T. Yanagida: Radiat. Meas. **112** (2018) 16.